Available online at www.sciencedirect.com

SCIENCE DIRECT®

Journal of Molecular Catalysis A: Chemical 202 (2003) 135–146

JOURNAL OF MOLECULAR CATALYSIS A: CHEMICAL

www.elsevier.com/locate/molcata

Dissociative adsorption and hydrodechlorination of CCl_4 on Ir(1 1 0)

C.T. Reeves, R.J. Meyer, C.B. Mullins*

Department of Chemical Engineering, 1 University Station C0400, University of Texas at Austin, Austin, TX 78712-0231, USA

Received 8 December 2002; accepted 21 February 2003

Abstract

The dissociative adsorption and hydrodechlorination of CCl_4 on a single crystal Ir(1 1 0) was investigated using temperature programmed desorption (TPD) and molecular beam techniques. In order to better understand the behavior of CCl_4, the adsorption and reactivity of less chlorinated methanes are compared to that of CCl_4. CCl_4 dissociates on the clean surface with near unity probability at low surface temperatures and decreases very slightly with increasing surface temperature. $CHCl_3$, CH_2Cl_2, and CH_3Cl also dissociate on the clean surface with near unity probability at low surface temperatures, however, the adsorption probability of these molecules are more sensitive to the surface temperature. As the molecule becomes less chlorinated, the adsorption probability falls more rapidly with increasing surface temperature. The preadsorption of hydrogen does not significantly affect the adsorption probability of CCl_4 or $CHCl_3$. However, with the β_2 adsorption state of hydrogen saturated, CH_2Cl_2 and CH_3Cl dissociatively adsorb with a small probability. Adsorption of CCl_4 on the hydrogen precovered surface was found to produce mainly $CHCl_3$ with trace amounts of CH_2Cl_2 and CH_4 (detected as CD_4). Similarly, adsorbed $CHCl_3$ will hydrodechlorinate to mainly CH_2Cl_2. Hydrodechlorination of CCl_4 is favored at lower surface temperatures and at higher surface coverages of dissociatively adsorbed CCl_4.

Keywords: Hydrodechlorination; Molecular beam techniques; Halogenated methanes

1. Introduction

Understanding the adsorption and interaction of halogenated methanes with surfaces is important for a number of reasons. The interaction of CCl_4 with iron surfaces [1–5] has been studied as a model system for understanding the tribological activity of chlorine-containing organics which are used as extreme pressure lubricant additives for use in the cutting and grinding of metals. CCl_4 has also been used as a model adsorbate in the study of photoinduced charge-transfer processes [6,7] in adsorbates on metal surfaces. Also, CCl_4, as well as many other halogenated organics, are atmospheric pollutants that are known to deplete the ozone layer.

Because CCl_4 has been labeled as an ozone depleting material by the Montreal Protocol [8], the production and use of CCl_4 has been discouraged. However, CCl_4 is still a significant component of many waste streams in the production of chlorinated organic compounds such as chloroform and dichloromethane [9]. Waste chlorocarbons are typically destroyed by thermal oxidation or catalytic oxidation [10] over supported metal catalysts such as Pt/alumina [11].

* Corresponding author. Tel.: +1-512-471-5817; fax: +1-512-471-7060.
E-mail address: mullins@che.utexas.edu (C.B. Mullins).

1381-1169/03/$ – see front matter © 2003 Elsevier Science B.V. All rights reserved.
doi:10.1016/S1381-1169(03)00197-3

Recently, hydrodechlorination of chlorocarbons over supported Group VIII metals (such as Ni, Pd, Rh, and Pt) [12–14] has been investigated as an alternative method of waste treatment [15–17]. Some of the advantages of hydrodechlorination over thermal or catalytic oxidation include the ability to reuse the reaction products, and minimal production of hazardous byproducts such as $COCl_2$. Unfortunately, many of these catalysts deactivate quickly and the chemistry of this deactivation is not well understood.

There are relatively few surface science studies of the adsorption of CCl_4 on metal surfaces and none address the interaction between adsorbed CCl_4 and hydrogen. On both the Fe(1 0 0) [18] and Fe(1 1 0) surfaces [1–4], dissociative adsorption is observed as well as the formation of $FeCl_2$ on the (1 1 0) surface. However, on the Cu(1 0 0) surface [19], dissociation is not detected and molecularly adsorbed CCl_4 desorbs at about 165 K. On the Ru(0 0 0 1) surface [20], temperature program desorption and electron stimulated desorption experiments indicate that at 100 K, CCl_4 adsorption is initially dissociative and adsorbs molecularly above about 13% of a monolayer. Similarly, on the Ni(1 1 0) surface [21], electron energy loss spectroscopy shows that at 110 K the initial adsorption is dissociative and becomes molecular at higher coverages. CCl_4 has also been shown to dissociate on the Ag(1 1 1) surface [6] at submonolayer coverages. Recently, CCl_4 has been shown to readily dissociate on the clean Ir(1 1 1) and Ir(1 1 0) surfaces [22,23] as well as on the oxygen precovered surfaces where it will react to produce $COCl_2$ (as well as CO and CO_2).

This paper focuses on the adsorption of CCl_4 on the clean and hydrogen precovered Ir(1 1 0) surface as well as the reaction of dissociatively adsorbed CCl_4 with preadsorbed hydrogen. In order to better understand the behavior of CCl_4, the adsorption and reactivity of $CHCl_3$, CH_2Cl_2, and CH_3Cl have also been investigated. The experimental techniques which were used include molecular beam reaction spectroscopy, temperature programmed desorption (TPD), and Auger electron spectroscopy.

2. Experimental

Experiments were performed in a molecular beam apparatus consisting of an ultra-high vacuum (UHV) scattering chamber, with a typical base pressure below 1.5×10^{-10} Torr, which is coupled to a differentially pumped molecular beam source. The UHV chamber is equipped with a quadrupole mass spectrometer (QMS), an Auger electron spectrometer, reverse-view low energy electron diffraction (LEED) optics, and an ion-sputtering gun. A more detailed description of the apparatus [24,25] has been reported previously.

The Ir(1 1 0) single crystal sample was mechanically polished within 0.3° of the (1 1 0) plane and mounted on a precision manipulator which allows accurate positioning of the sample and adjustment of the angle of the surface relative to the molecular beam. The sample can be heated to 1800 K by resistive heating of 0.010 in. Ta wires spot welded to the sides of the sample. These wires are also in good thermal contact with a liquid nitrogen reservoir, which allow the sample to be cooled to 77 K. The sample temperature was monitored by a type C thermocouple spot welded to the bottom edge of the sample.

The sample was initially cleaned by argon ion sputtering and annealing cycles. Any remaining carbon contamination was removed by repeated cycles of adsorbing oxygen at 77 K and annealing to 1600 K in vacuum. This treatment resulted in a surface free of contamination within the limits of the Auger spectrometer. Oxygen adsorption followed by vacuum annealing to 1600 K was routinely used to clean the sample between experiments.

The structure of the clean Ir(1 1 0) surface is still a subject of debate [26]. The LEED pattern obtained suggests a corrugated (3 3 1) mesoscopically faceted structure [26–28], which has been studied previously using LEED and STM. A corrugated (1×2) missing row reconstruction [29,30] and a corrugated mixed $(1 \times 3)/(1 \times 1)$ reconstruction [31,32] have also been reported, although these reconstructions may be stabilized by impurities. Each of these surface structures are similar in that they present (1 1 1) "microfacets" consisting of highly coordinated atoms and a number of less coordinated atoms at the edge or intersection of these microfacets.

Mildly supersonic beams of CCl_4, $CHCl_3$, and CH_2Cl_2 were produced by expanding pure vapor, taken from the vapor space of a reservoir of liquid (99.9%, Aldrich), through a 70 μm orifice into vacuum. The liquid reservoir was held at room temperature when using CCl_4. The liquid reservoir was

immersed in an ice–water bath when using $CHCl_3$ and CH_2Cl_2 in order to lower the vapor pressure of the liquid. The vapor pressures of the liquids are estimated to be 113 Torr for CCl_4, 59 Torr for $CHCl_3$, and 143 Torr for CH_2Cl_2 at the specified operating temperature. The liquid chloromethanes were thoroughly degassed before use by mechanically pumping on the vapor space of the reservoir until no dissolved gases could be detected in the molecular beam by the mass spectrometer. Supersonic beams of CH_3Cl were produced from CH_3Cl gas dilutely seeded in an argon carrier gas. This gas mixture was expanded through the 70 μm orifice with an upstream pressure of 17 psia. The translational energy distributions of the chlorocarbon beams were measured using standard time-of-flight techniques [33]. The average translational energy of the molecular beam was 0.10 eV for CCl_4, 0.09 eV for $CHCl_3$, 0.09 eV for CH_2Cl_2, and 0.08 eV for CH_3Cl. The spread of the translational energy distribution, $\Delta E/E$ (where ΔE is the full-width at half-maximum), was measured to be 1.0 for CCl_4, $CHCl_3$, and CH_2Cl_2, and 0.2 for CH_3Cl. The flux of the beam was determined from the pressure rise in the chamber when the beam is scattered from an inert surface employing the ionization sensitivity factor for the molecule of interest.

3. Results and discussion

3.1. Temperature programmed desorption of CCl_4

Temperature programmed desorption was used to investigate the adsorption state(s) of CCl_4 on the Ir(1 1 0) surface. Fig. 1 shows the desorption spectra of CCl_4 as a function of the CCl_4 exposure. The desorption spectra were obtained by exposing the surface to a specified amount of CCl_4 at a surface temperature below 110 K and then subsequently heating the surface at a rate of 3 K/s while monitoring mass 47 with the quadrupole mass spectrometer. Mass 47 (CCl^+) was used to monitor the desorption of CCl_4 because the mass spectrometer in our system is most sensitive to this cracking fragment of CCl_4. CCl_4 was delivered to the surface of the single crystal sample using a molecular beam in order to minimize the exposure of other surfaces within the chamber including the back of the single crystal sample (which is known

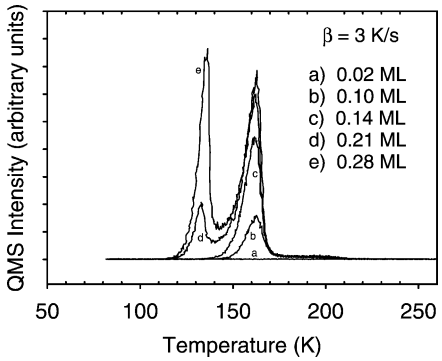

Fig. 1. Temperature programmed desorption of CCl_4 from Ir(1 1 0). Mass 47 (CCl^+) was used to monitor the desorption of CCl_4 at a heating rate of 3 K/s.

to have a larger concentration of defects). Coverages were determined from the flux of the beam and the exposure time of the sample to the beam (at 110 K the adsorption probability is 100%). Exposure of these other surfaces lead to spurious peaks in the desorption spectra.

At low exposures of CCl_4, no CCl_4 desorbs, indicating that adsorption of CCl_4 is dissociative at low surface coverages. As the CCl_4 exposure increases, molecular CCl_4 is seen to desorb from the surface around 165 K. Using the Redhead [34] analysis, this peak desorption temperature gives an adsorption energy of 0.43 eV. Here, molecular CCl_4 is desorbing from a surface partially covered with dissociated CCl_4. As the CCl_4 exposure is further increased, a second desorption state is observed at around 135 K. This is CCl_4 desorbing from a second layer or multilayer of molecularly adsorbed CCl_4. The temperature programmed desorption spectrum of CCl_4 on Ir(1 1 0) is similar to that of CCl_4 on the Fe(1 1 0) [1], Ru(0 0 0 1) [20], and Ir(1 1 1) surfaces. On the Fe(1 1 0) surface, CCl_4 desorption features are seen at 140 K (multilayer) and 154 K (first layer). On the Ru(0 0 0 1) surface, desorption is observed at 185 K (first layer); 165, and 145 K (multilayer). CCl_4 thermally desorbs from Ir(1 1 1) [35] with features at 135 K (multilayer) and 165 K (first layer) with a shoulder extending out to 180 K.

The formation of trace amounts of C_2Cl_4 was detected during the temperature programmed desorption of CCl_4. Masses 94 ($C_2Cl_2^+$), 129 ($C_2Cl_3^+$), and 166

($C_2Cl_4^+$) were detected at about 200 K indicating the formation of C_2Cl_4. Masses 94, 129, and 166 are also major cracking fragments of C_2Cl_6, however, mass 201 ($C_2Cl_5^+$) was not detected. Therefore, C_2Cl_6 is not believed to be produced during the temperature programmed desorption of CCl_4 in a detectable quantity. The formation of C_2Cl_4 from CCl_4 has been reported by Smentkowski et al. on the Fe(1 1 0) [1–3] surface (two desorption features at 177 and 198 K) and also by Dixon-Warren et al. on the Ag(1 1 1) [6] surface (desorbing at 270 K).

Adsorbed chlorine, left from the dissociative adsorption of CCl_4, is observed to desorb from the surface upon heating. However, the exact form in which it leaves is still unclear. When the surface is saturated with dissociatively adsorbed CCl_4 and then heated to 1600 K, desorption of Cl_2 from the surface is not detected by the mass spectrometer at mass 70 (Cl_2^+). However, with the front of the sample directly facing the mass spectrometer, mass 35 (Cl^+) is observed to desorb from the surface in a peak centered around 1100 K (with no corresponding mass 70 signal). This mass 35 signal is possibly from the desorption of Cl atoms. The desorption of some molecular chlorine cannot be ruled out since it is known that the walls of the vacuum chamber will very readily adsorb Cl_2, making the detection of small amounts of Cl_2 difficult. Auger electron spectroscopy was also used to monitor Cl loss from the surface. As seen in Fig. 2, Auger electron spectroscopy shows that as the surface is heated, a small amount of Cl leaves the surface between 600 and 700 K and then the remaining Cl leaves between 800 and 1200 K. This behavior is consistent with the results of Schennach and Bechtold [36], who investigated the adsorption and desorption of chlorine from the Pt(1 1 0) surface. Schennach and Bechtold report that chlorine desorbs from the Pt(1 1 0) surface in two forms: as molecular chlorine between about 600 and 800 K and as atomic chlorine between about 800 and 1050 K. They also report that from maximum initial-concentration adlayers, about 2/9 of the adsorbed chlorine atoms desorb as molecular chlorine with the remainder desorbing as atoms. This ratio is consistent with the Auger measurements shown in Fig. 2, where approximately 2/9 of the chlorine is lost from the surface between 600 and 800 K. Desorption of iridium chlorides was not observed. Desorption of iron chloride has been observed from CCl_4 adsorbed on Fe(1 1 0) [1–4], however, Schennach and Bechtold report that no platinum chloride is produced during the thermal desorption of chlorine from Pt(1 1 0) and Pt(1 1 1).

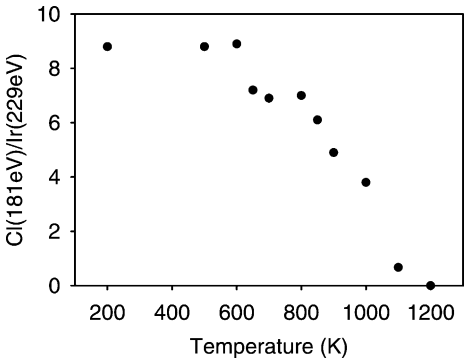

Fig. 2. The desorption of chlorine from the surface was monitored using Auger electron spectroscopy. The surface was saturated with CCl_4 at 200 K then flashed to a specified temperature at 10 K/s. After heating, the Cl concentration was monitored using Auger electron spectroscopy. The relative Cl concentration is given by the ratio of the Cl 181 eV peak-to-peak amplitude to the Ir 229 eV peak-to-peak amplitude.

3.2. *Initial adsorption probability of CCl_4 on clean Ir(1 1 0) as compared with $CHCl_3$, CH_2Cl_2 and CH_3Cl*

The initial adsorption probabilities of CCl_4, $CHCl_3$, CH_2Cl_2, and CH_3Cl on the clean Ir(1 1 0) surface were measured (Fig. 3) as a function of the surface temperature and incident angle using a reflectivity technique

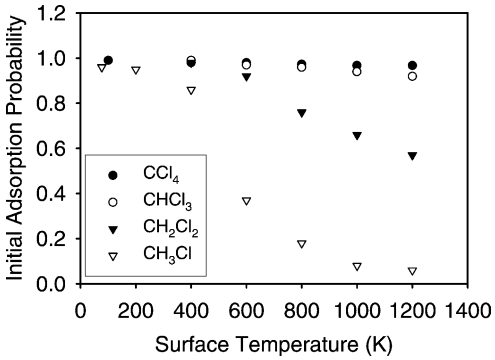

Fig. 3. Initial adsorption probabilities for CCl_4 and CH_3Cl as a function of surface temperature. The standard deviation of each measurement is ±0.03.

similar to that first demonstrated by King and Wells [37–39]. In this type of experiment, the QMS signals from the beam impinging upon the sample and upon an inert flag are compared. The initial dissociative adsorption probability can be determined from the ratio of these signals provided that the exposure time is small compared to the time needed to saturate the surface.

The initial adsorption probability for all of these molecules decreases as the surface temperature is increased from 100 to 1200 K. However, this surface temperature dependence is weak for CCl_4 and becomes stronger as the chloromethane becomes less chlorinated.

Most measurements were made with the molecular beam incident at 60° from the surface normal. Changing the incident angle from normal incidence to 60° had no measurable effect on the adsorption probabilities. This behavior is consistent with adsorption proceeding mainly through a precursor-mediated mechanism [40–42] where the molecule first molecularly adsorbs into a mobile precursor state before dissociatively chemisorbing. Frequently, in a direct dissociation channel, the adsorption is strongly dependent on the normal component of the incident molecules momentum, such that a significant decrease in the adsorption probability would be expected when the incident angle of the molecular beam is changed from normal incidence to 60° incidence if the direct mechanism was playing a significant role. We assume here that the mechanism of adsorption is precursor mediated.

The temperature dependence of the initial adsorption probability can also be understood as a consequence of precursor-mediated adsorption and the details of the potential energy surface. In precursor-mediated adsorption, the surface temperature dependence of the initial adsorption probability is controlled by the difference between the energy barrier to desorption from the molecularly adsorbed state (E_d) and the energy barrier to dissociative chemisorption from the molecularly adsorbed state (E_c), as well as the ratio of the pre-exponential for desorption to that for chemisorption (ν_d/ν_c) as shown in Eqs. (1) and (2), where α is the molecular adsorption probability, k_c is the rate constant for chemisorption, k_d is the rate constant for desorption, and T_s is the surface temperature.

$$S_0 = \alpha \frac{k_c}{k_c + k_d} = \alpha \frac{1}{1 + (k_d/k_c)} \quad (1)$$

$$S_0 = \alpha \frac{1}{1 + (\nu_d/\nu_c)\exp[(E_d - E_c)/kT_s]} \quad (2)$$

Based on Eq. (2), the decrease in adsorption probability with increasing surface temperature for each of the chloromethanes studied is indicative of precursor-mediated adsorption, where the barrier to desorption from the molecularly adsorbed state is greater than the barrier to dissociative chemisorption. This condition is expected to be true for all of the chloromethanes studied. The C–Cl bond strength in all of these compounds is relatively weak while the molecular adsorption energy is high due to the strong van der Waals forces between the metal surface and the highly polarizable molecules. The energy barrier to desorption from the clean surface could not be measured by TPD because all of these molecules readily dissociate on the clean surface. However, on partially covered surfaces the desorption energies of all of these molecules are around 0.4 eV and the desorption energy from the clean surface is assumed to be near that value. Because the desorption energy is much greater than kT_s, all of these molecules have long lifetimes on the surface, relative to a vibrational period, even at high surface temperatures (~200 ps at 600 K).

If $E_d - E_c$ is much larger than kT_s, then the adsorption probability will be nearly independent of surface temperature. This condition is expected to be true for CCl_4, which has a very weak bond to break (small E_c) and a large molecular adsorption energy (large $E_d \gg kT_s$). As $E_d - E_c$ gets smaller, the adsorption probability will become more sensitive to the surface temperature. This will occur if E_c increases or if E_d decreases.

As seen in Fig. 3, the effect of surface temperature on the adsorption probability becomes stronger as the molecule becomes less chlorinated. This trend is directly correlated with the C–Cl bond strength in each of these molecules. As the number of Cl atoms in the molecule decreases, the C–Cl bond strength [43] increases (3.17 eV for CCl_4, 3.45 eV for $CHCl_3$, 3.63 eV for CH_2Cl_2, 3.69 eV for CH_3Cl). This increase in bond strength will likely increase the barrier to dissociative chemisorption (E_c) which would in turn cause $E_d - E_c$ to decrease.

Note, however, that changes in E_d as well as ν_d/ν_c will also affect the dependence of the adsorption probability on surface temperature. We would expect the ratio of pre-exponentials to be different for each molecule due to steric effects. For example while CCl_4 has four equivalent C–Cl bonds, CH_3Cl has only one C–Cl bond to break. These molecules also have different dipole moments [44] (0 D for CCl_4, 1.2 D for $CHCl_3$, 1.62 D for CH_2Cl_2, and 1.87 D for CH_3Cl), which may interact with the surface dipole and affect the ratio of pre-exponentials or even the energies barriers to desorption and chemisorption.

By fitting the data shown in Fig. 3 to Eq. (2), the values of $E_d - E_c$ and ν_d/ν_c can be found for each system. Because the adsorption probabilities for CCl_4 and $CHCl_3$ do not change much over the temperature range studied it is difficult to fit this data accurately since several combinations of $E_d - E_c$ and ν_d/ν_c will give reasonable fits to the data, although the values of the parameters may not be physically realistic. Therefore, we have fit the data to Eq. (2) to estimate $E_d - E_c$ with the constraint that ν_d/ν_c is greater than or equal to 1. This ratio is expected to be greater than unity because the phase space for desorption should be greater than the phase space for adsorption. For CCl_4, $E_d - E_c$ is estimated to be greater than 0.4 eV with ν_d/ν_c greater than or equal to 1. For $CHCl_3$, $E_d - E_c$ is estimated to be greater than 0.26 eV with ν_d/ν_c greater than or equal to 1. For CH_2Cl_2, $E_d - E_c$ was found to be 0.20 eV with ν_d/ν_c equal to 5. For CH_3Cl, $E_d - E_c$ was found to be 0.25 eV with ν_d/ν_c equal to 186. The relative magnitudes of ν_d/ν_c are consistent with the intuitive notion that the transition state for reaction becomes more constrained as the molecule is less chlorinated, while the transition state for desorption would be much less influenced.

3.3. Uptake of CCl_4 on Ir(1 1 0)

Fig. 4 shows the uptake of CCl_4 on the Ir(1 1 0) surface. The saturation coverage of CCl_4 was determined to be 0.08 ± 0.03 ML at a surface temperature of 200 K (1 ML $\equiv 9.6 \times 10^{14}$ molecules/cm^2). In these experiments, a molecular beam of CCl_4 impinges on a clean Ir(1 1 0) surface held at the specified surface temperature and the reflected (non-adsorbed) CCl_4 is detected by the mass spectrometer. At 70 s, a shutter is opened allowing the molecular beam to enter the scattering chamber and impinge on the sample. As the sample accumulates dissociatively adsorbed CCl_4, the surface becomes poisoned and less CCl_4 adsorbs (more CCl_4 reflects) and the reflected CCl_4 mass spectrometer signal increases. At 120 s, an inert flag is inserted just in front of the sample, blocking the molecular beam. As the molecular beam strikes the inert flag, all of the

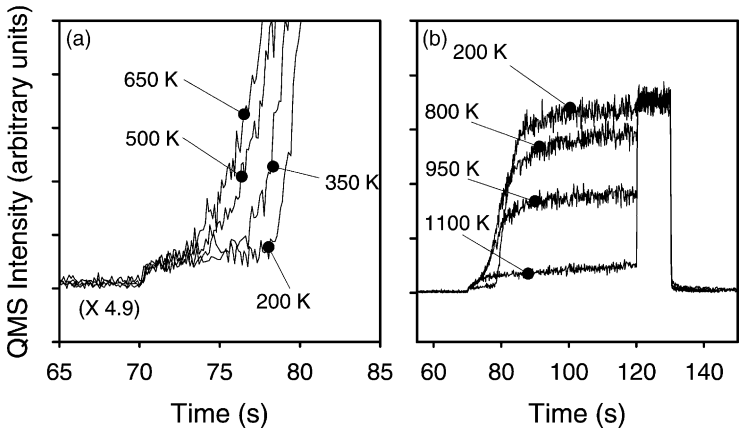

Fig. 4. Uptake of CCl_4 on the Ir(1 1 0) surface. Panel (a) shows a detailed view of the initial adsorption of CCl_4 between 200 and 650 K. Panel (b) shows the adsorption of CCl_4 for surface temperatures between 200 and 1100 K. The molecular beam enters the scattering chamber and begins to impinge on the surface at 70 s. At 120 s, an inert flag is placed in front of the sample causing the entire molecular beam to reflect from the flag. At 130 s, the molecular beam is stopped from entering the scattering chamber.

molecules in the beam are reflected from the flag and the mass spectrometer then reads a signal proportional to the total number of molecules striking the sample. At 130 s, the beam shutter is closed and the molecular beam no longer enters the scattering chamber and the mass spectrometer signal drops back to the baseline.

At a surface temperature of 200 K, the adsorption probability stays near unity and does not change significantly until the surface is almost saturated with dissociatively adsorbed CCl_4. This behavior is indicative of a precursor-mediated adsorption mechanism as described previously. Adsorption through a precursor channel allows the molecule to migrate across the surface and find an unoccupied site available for dissociative adsorption whereas in a direct mechanism adsorption could only take place if the initial site of impact was unoccupied. Therefore, adsorption through a direct mechanism would be more surface coverage dependent than is seen here.

These uptake curves also show that initially, in the limit of zero adsorbed CCl_4 the adsorption probability is independent of the surface temperature but as the surface accumulates dissociatively adsorbed CCl_4, the adsorption probability becomes more dependent on the surface temperature. This behavior is likely due to the change in the energy barrier to C–Cl bond cleavage as the surface accumulates Cl onto the surface. As dissociated CCl_4 accumulates on the surface, the adsorbed chlorine will increase the work function [18,45] of the surface, which may in turn increase the energy barrier to dissociation of the C–Cl bond in CCl_4. The presence of chlorine on the surface may also lower E_d increasing the probability of desorption. In either case as Cl accumulates on the surface, $E_d - E_c$ will decrease and therefore, the adsorption probability will be more sensitive to the surface temperature.

Uptake curves at higher surface temperatures (>800 K) show that the adsorption probability can remain very high even after an exposure of CCl_4 that would saturate the surface at lower temperatures. This effect is due to desorption of Cl from the surface at the higher surface temperatures. As the surface temperature increases, the desorption rate of Cl increases and the steady-state coverage of Cl on the surface will decrease. As the Cl coverage decreases the adsorption probability increases. At 1100 K, there is little Cl on the surface as CCl_4 is adsorbed and the adsorption probability remains high. The adsorption probability does decrease slowly over time however, due to the accumulation of carbon on the surface, which does not desorb.

3.4. Adsorption and reaction of CCl_4 on H-precovered Ir(1 1 0)

The adsorption and desorption of hydrogen from the Ir(1 1 0) surface has been studied previously using temperature programmed desorption and contact potential difference techniques [46]. Hydrogen desorption measurements from the sample used in this study agree with the previously reported measurements. Temperature programmed desorption of hydrogen shows two desorption states: a β_1 state desorbing around 200 K and a β_2 state desorbing around 375 K. The β_1 state is believed to be hydrogen adsorbed on sites associated with the highly coordinated atoms that make up the (1 1 1) microfacets of the surface reconstruction. The β_2 state is believed to be hydrogen adsorbed on sites associated with the less coordinated atoms[1] [47] on the surface. Because the β_2 state adsorption site is associated with highly uncoordinated atoms, these sites bind hydrogen more strongly than the β_1 sites, as indicated by the higher desorption temperature in the temperature programmed desorption. This low degree of coordination is also believed to be responsible for the high activity of the β_2 state sites, relative to the β_1 state sites, toward the dissociation of H_2 and small alkanes [48]. The initial dissociative chemisorption probability [46] of H_2 on the β_2 sites is near unity while the chemisorption probability on the β_1 sites is on the order of 10^{-2}. It has also been shown that adsorbing H into the β_2 sites of Ir(1 1 0) will block the dissociation of small alkanes, causing the surface to have a reactivity similar to the close packed (1 1 1) surface [48].

In order to investigate the effect of hydrogen coverage on the adsorption of CCl_4, initial adsorption probability measurements were made with the β_2 sites saturated with hydrogen. In the temperature range of 170–250 K, the adsorption probability is 0.96 ± 0.03, which is just slightly less than the adsorption probability measured on the clean surface. This result

[1] Due to the similarity in the hydrogen TPD, we expect hydrogen adsorbed on Ir(1 1 0) to occupy similar sites to those on the Pt(1 1 0) surface.

indicates that the remaining β_1 sites are active enough to readily dissociate the C–Cl bond in CCl_4. This idea is consistent with the results of Meyer et al. where CCl_4 is shown to adsorb with near unity probability at low surface temperatures on the Ir(1 1 1) surface [35] (which consists of β_1 type sites only). However, we have shown that if the β_2 state of hydrogen is saturated, the adsorption probabilities of CH_2Cl_2 and CH_3Cl drop to 0.01 ± 0.03 and 0.02 ± 0.03, respectively, at a surface temperature of 250 K compared to 0.99 ± 0.03 and 0.96 ± 0.03, respectively, on the clean surface. The adsorption probability of $CHCl_3$ remains high, dropping only to 0.94 ± 0.03 compared to 0.99 ± 0.03 on the clean surface. These results indicate that on the Ir(1 1 0) surface, with hydrogen saturating the β_2 sites, the available β_1 sites can dissociate the relatively weak C–Cl bond in CCl_4, but are not reactive enough to break the stronger C–Cl bond in CH_2Cl_2 or CH_3Cl.

Adsorbed CCl_4 will react readily with preadsorbed hydrogen to form several hydrodechlorination products. $CHCl_3$ is the major product formed. CH_2Cl_2 and CH_4 are also produced in trace amounts. The production of CH_3Cl could not be detected. Figs. 5 and 6 show typical experiments in which hydrodechlorination products were detected by the mass spectrometer as a molecular beam of CCl_4 was allowed to impinge on the Ir(1 1 0) surface which had been predosed with enough hydrogen to saturate the β_2 state sites. Note that the signals in Figs. 5 and 6 have been scaled to take into account differences in the mass spectrometer sensitivity, pumping speed, and ion gauge sensitivity for each species. At 70 s, a shutter is opened to allow the molecular beam to enter the scattering chamber and impinge on the sample. The beam is allowed to impinge on the sample for 50 s and then the beam shutter is closed at 120 s stopping the beam from entering the scattering chamber. At a surface temperature of 200 K (Fig. 5), the adsorption probability of CCl_4 is initially 0.96 and remains high for about 10 s. During this time only a small amount of the incident CCl_4 is reflected from the surface and detected by the mass spectrometer at mass 117 (CCl_3^+). Although the mass spectrometer used in this study was most sensitive to the mass 47 (CCl^+) fragment of CCl_4, mass 117 was used to monitor for CCl_4 since mass 117 was not a major cracking fragment of other hydrodechlorination products formed. After about 10 s of exposure the surface begins to saturate with dissociatively adsorbed CCl_4 and a corresponding rise of the reflected

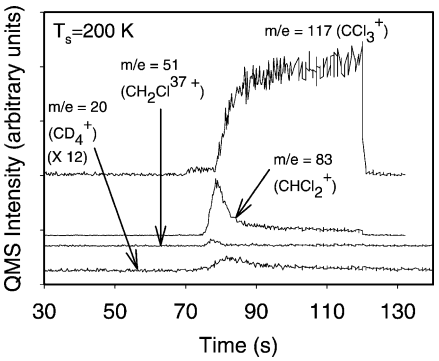

Fig. 5. King and Wells measurement of the adsorption and reaction of CCl_4 on the hydrogen (deuterium) precovered Ir(1 1 0) surface at 200 K. The hydrogen (deuterium) coverage is that which saturates the β_2 state. The molecular beam of CCl_4 starts to impinge on the surface at 70 s and stops at 120 s. The production of $CHCl_3$, CH_2Cl_2, and CD_4 (using deuterium in a separate experiment) were monitored using masses 83, 51, and 20, respectively. The production of CH_3Cl could not be detected. The different QMS signals have been vertically displaced from one another for clarity. The signals shown have been scaled to take into account the sensitivity of the mass spectrometer toward the different species as well as differences in pumping speeds and ion gauge sensitivities. The mass 20 signal has also been magnified by a factor of 12.

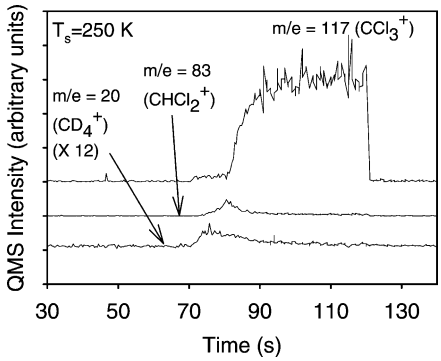

Fig. 6. King and Wells measurement of the adsorption and reaction of CCl_4 on the hydrogen (deuterium) precovered surface Ir(1 1 0) surface at 250 K. The conditions are identical to that shown in Fig. 5 except for the surface temperature. The different QMS signals have been vertically displaced from one another for clarity. The signals shown have also been scaled to take into account the sensitivity of the mass spectrometer toward the different species as well as differences in pumping speeds and ion gauge sensitivities. The mass 20 signal has also been magnified by a factor of 12.

CCl_4 signal is seen. This signal eventually levels off as the surface becomes saturated, at which point all of the incoming CCl_4 is reflected from the surface. At 120 s, the beam shutter is closed and the CCl_4 signal drops back to the baseline level.

The production of $CHCl_3$ was detected by the mass spectrometer at mass 83, which is the $CHCl_2^+$ cracking fragment. A fragment of this mass is not produced in any significant amount by CCl_4 or any of the other hydrodechlorination products. At a surface temperature of 200 K (Fig. 5), $CHCl_3$ is not produced immediately as the CCl_4 beam impinges on the sample. Not until the surface starts to become saturated with adsorbed CCl_4, and the adsorption probability of CCl_4 begins to drop, does $CHCl_3$ begin to be produced. The production of $CHCl_3$ increases as adsorbed CCl_4 further poisons the surface. Eventually the $CHCl_3$ production goes through a maximum and then decreases as the production rate of $CHCl_3$ becomes limited by the decreasing adsorption probability of CCl_4.

The fact that $CHCl_3$ is not produced immediately as the CCl_4 beam impacts the sample indicates that some amount of dissociatively adsorbed CCl_4 must accumulate on the surface before $CHCl_3$ can be produced. As Cl from the dissociatively adsorbed CCl_4 accumulates on the surface, the activity of the surface toward C–Cl bond cleavage is likely reduced concomitant with an increase in the work function of the surface. This reduced activity may stabilize the adsorbed CCl_3 species of dissociatively adsorbed CCl_4 allowing it to react with adsorbed hydrogen to form $CHCl_3$ whereas on the clean surface, the CCl_3 will perhaps be decomposed too rapidly to form $CHCl_3$. In fact, if Cl from Cl_2 is preadsorbed on the surface along with hydrogen, $CHCl_3$ formation will occur almost immediately after the CCl_4 beam is allowed to hit the surface.

CH_2Cl_2 is also produced at a surface temperature of 200 K (Fig. 5). Production of CH_2Cl_2 was monitored by the mass spectrometer at a mass of 51 (CH_2Cl^{37+}). Fragments of mass 51 are not significantly produced by any of the other species discussed. Mass 49, which is the major cracking fragment of CH_2Cl_2 (CH_2Cl^+) could also be detected, however this is the same mass as a significant cracking fragment of CCl_4 and $CHCl_3$ (CCl^{37+}). Subtracting the contribution to the mass 49 signal from CCl_4 and $CHCl_3$ (both from CCl^{37+}), gives a residual mass 49 signal that would be expected from CH_2Cl_2 based on the mass 51 signal. Production of CH_2Cl_2 was confirmed by preadsorbing deuterium in place of hydrogen. Using deuterium, masses 51 (CD_2Cl^+) and 53 (CD_2Cl^{37+}) were detected consistent with the cracking pattern expected for CD_2Cl_2.

The production of CH_3Cl was monitored using mass 52 (CH_3Cl^{37+}). Although the mass spectrometer is most sensitive to the parent mass 50 signal for CH_3Cl, $CHCl_3$ also produces a significant mass 50 signal from the $HCCl^{37+}$ fragment. Mass 52 was not detected for experiments performed at surface temperatures between 170 and 250 K. Therefore, we believe that CH_3Cl is not produced in a detectable amount.

Due to the relatively high background of mass 16 in our vacuum chamber, it was not possible to detect small amounts of CH_4 produced. However, when deuterium was substituted for hydrogen, the presence of mass 20 (CD_4^+) could be detected. It should be noted that the detection limit of CD_4 in our system is about an order of magnitude greater than that of any of the other chlorinated species discussed. This is mainly due to the cold surfaces within our system which pump the chlorinated species very well compared to CD_4, which will not condense on those cold surfaces.

The effect of surface temperature on the production of $CHCl_3$ was also investigated. Fig. 6 shows that if the surface temperature is increased from 200 to 250 K (Fig. 5), the production of $CHCl_3$ is dramatically reduced. This decrease in $CHCl_3$ production is likely due to an increase in the rate of decomposition of the surface CCl_3 species at higher surface temperatures, which lowers the likelihood of a CCl_3 species reacting with adsorbed hydrogen before it further decomposes. The production of CH_2Cl_2 is also reduced at higher surface temperatures. The production of CD_4 at a surface temperature of 250 K was approximately the same as that at 200 K. Decreasing the surface temperature from 200 to 170 K, had no significant effect on the production of $CHCl_3$, however, at this lower temperature, no CH_2Cl_2, CH_3Cl, or CD_4 was detected. At this low temperature, it is possible that the rate of reaction between surface intermediates (CH_xCl_y (ads)) and hydrogen needed to form these compounds becomes negligible.

The effect of hydrogen coverage on $CHCl_3$ production was also investigated (Fig. 7). For hydrogen coverages below the β_2 saturation coverage, the production of $CHCl_3$ was very low. At a surface temperature of 170 K, the production of $CHCl_3$ does not

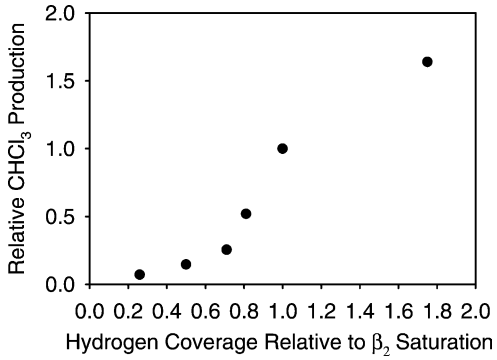

Fig. 7. Effect of hydrogen coverage on the production of $CHCl_3$. The relative $CHCl_3$ production has been normalized by the $CHCl_3$ production when the β_2 state of hydrogen is saturated. The hydrogen coverage has also been presented relative to the coverage where the β_2 state is saturated.

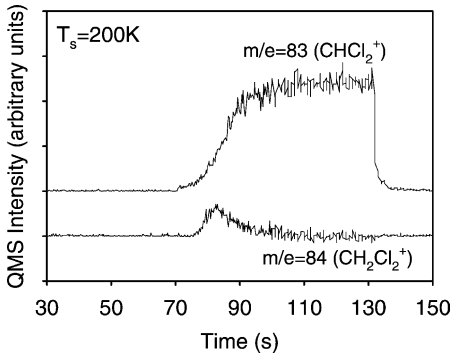

Fig. 8. King and Wells measurement of the adsorption and reaction of $CHCl_3$ on the hydrogen precovered surface Ir(1 1 0) surface at 200 K. The molecular beam impinges on the surface between 70 and 130 s. A small part of the mass 84 signal, which is due to a cracking fragment of $CHCl_3$, has been subtracted out. The different QMS signals have been vertically displaced from one another for clarity. The signals shown have also been scaled to take into account the sensitivity of the mass spectrometer toward the different species as well as differences in pumping speeds and ion gauge sensitivities.

become significant until the hydrogen coverage nears that necessary to saturate the β_2 state. This result indicates that the β_2 sites may decompose the surface CCl_3 species too quickly for it to react with surface hydrogen to form $CHCl_3$. Once the β_2 state of hydrogen is saturated, and those sites are effectively blocked, then the β_1 sites will still be able to dissociatively adsorb CCl_4 leaving CCl_3. However, the β_1 sites likely decompose the CCl_3 species less rapidly than the β_2 sites, allowing the CCl_3 species time to react with hydrogen to produce $CHCl_3$. At hydrogen coverages above the β_2 saturation coverage, $CHCl_3$ production increases roughly linearly with the hydrogen coverage up to 1.8 times the β_2 saturation coverage which was the highest hydrogen coverage studied.

As noted above, when the β_2 sites are saturated with hydrogen, CH_2Cl_2 and CH_3Cl will no longer adsorb while $CHCl_3$ still adsorbs with a probability of 0.94. We have seen that upon adsorption on the Ir(1 1 0) surface, with the β_2 state of hydrogen saturated, $CHCl_3$ will hydrodechlorinate similarly to CCl_4 (Fig. 8). At 200 K, $CHCl_3$ will react with adsorbed hydrogen to produce mainly CH_2Cl_2. CH_2Cl_2 production was monitored using mass 84 ($CH_2Cl_2^+$). Similar to the hydrodechlorination of CCl_4, the production of CH_2Cl_2 from $CHCl_3$ does not become significant until some amount of dissociated $CHCl_3$ has accumulated on the surface, causing the surface to become less active toward C–Cl bond cleavage. The production of CH_3Cl was not detected and the production of CH_4 is questionable. Although CHD_3 could be detected when preadsorbing deuterium instead of hydrogen, the production of mass 19 (CHD_3^+) was near the detection limit of the QMS. When the surface temperature is raised to 250 K, the production of CH_2Cl_2 decreases to approximately 1/3 of that produced at 200 K. This indicates that as the surface temperature is raised, the $CHCl_2$ surface intermediate becomes less stable and is more likely to decompose than react with adsorbed hydrogen to produce CH_2Cl_2.

4. Conclusions

Carbon tetrachloride was found to dissociatively adsorb on the clean Ir(1 1 0) surface with a probability of 0.99 at low surface temperatures which decreases slightly to 0.97 as the temperature is increased to 1200 K. Other less chlorinated methanes, such as $CHCl_3$, CH_2Cl_2, and CH_3Cl also dissociate with near unity probability at low surface temperatures and their adsorption probability also decreases with increasing surface temperature. The adsorption probability becomes more sensitive to the surface temperature as the molecule becomes less chlorinated. This behavior is possibly due to an increase in the C–Cl bond strength

as the molecule becomes less chlorinated. Adsorption is believed to occur though a precursor-mediated mechanism for all of the chloromethanes investigated. Studies of the uptake of CCl_4 indicate that as Cl is accumulated on the surface, the adsorption probability of CCl_4 becomes more sensitive to the surface temperature. This increased surface temperature dependence is possibly due to an increase in the work function of the surface, which in turn increases the energy barrier to C–Cl bond cleavage.

The adsorption of hydrogen does not significantly affect the adsorption probability of CCl_4 (or $CHCl_3$) at low surface temperatures. However, when the β_2 state of hydrogen is saturated, CH_2Cl_2 and CH_3Cl will not significantly dissociatively adsorb. Adsorbed hydrogen can react with dissociatively adsorbed CCl_4 to produce mainly $CHCl_3$ with trace amounts of CH_2Cl_2 and CH_4 (detected as CD_4). The production of $CHCl_3$ was favored at lower surface temperatures where the CCl_3 intermediate is less likely to be decomposed before reacting with adsorbed hydrogen. $CHCl_3$ production is also favored at higher Cl coverages, possibly due to Cl reducing the activity of the surface toward the decomposition of the CCl_3 intermediate. It is also noted that $CHCl_3$ production is not significant until the β_2 state of hydrogen is nearly saturated. This behavior indicates that the highly active β_2 sites may decompose the CCl_3 species too rapidly to produce $CHCl_3$. Similarly, $CHCl_3$ has been shown to hydrodechlorinate to CH_2Cl_2.

Acknowledgements

The authors gratefully acknowledge support of this work from the Welch Foundation (Grant No. F-1436), the Gulf Coast Hazardous Substances Research Center (Grant No. 069UTA0802), and the donors of the Petroleum Research Fund, administered by the American Chemical Society.

References

[1] V.S. Smentkowski, C.C. Cheng, J.T. Yates Jr., Langmuir 6 (1990) 147.
[2] V.S. Smentkowski, J.T. Yates Jr., Surf. Sci. 232 (1990) 102.
[3] V.S. Smentkowski, C.C. Cheng, J.T. Yates Jr., Surf. Sci. Lett. 215 (1989) L279.
[4] V.S. Smentkowski, M.D. Ellison, J.T. Yates Jr., Surf. Sci. 235 (1990) 116.
[5] J. Lara, H. Molero, A. Ramirez-Cuesta, W.T. Tysoe, Langmuir 12 (1996) 2488.
[6] St.J. Dixon-Warren, E.T. Jensen, J.C. Polanyi, J. Chem. Phys. 98 (1993) 5938.
[7] St.J. Dixon-Warren, E.T. Jensen, J.C. Polanyi, Phys. Rev. Lett. 67 (1991) 2395.
[8] Montreal Protocol on Substances that Deplete the Ozone Layer, Final Report, United Nations Environment Program, New York, 1987.
[9] G.M. Wells, Handbook of Petrochemicals and Processes, second ed., Ashgate, Brookfield, 1999, pp. 148–304.
[10] B.K. Hodnet, Heterogeneous Catalytic Oxidation: Fundamental and Technological Aspects of the Selective and Total Oxidation of Organic Compounds, Wiley, New York, 2000, pp. 285–300.
[11] Y. Wang, H. Shaw, R.J. Farrauto, Catalytic oxidation of trace concentrations of trichloroethylene over 1.5% platinum on alumina, ACS Adv. Chem. Symp. Ser. 495 (1992) 125.
[12] A.H. Weiss, K.A. Krieger, J. Catal. 6 (1966) 167.
[13] A.L. Weiss, B.S. Gambhir, R.B. Leon, J. Catal. 22 (1971) 245.
[14] D.I. Kim, D.T. Allen, Ind. Eng. Chem. Res. 36 (1997) 3019.
[15] L.N. Ito, C.B. Murchison, M.T. Holbrook, A.D. Harley, D.D. Smith, Process for Converting Chlorinated Alkenes to Useful Less Chlorinated Alkenes, United States Patent 5,476,979 (1995).
[16] A.D. Harley, M.T. Holbrook, D.D. Smith, M.D. Cisneros, L.N. Ito, C.B. Murchison, Processes for Converting Chlorinated Byproducts and Waste Products to Useful Materials, United States Patent 5,453,557 (1995).
[17] T.N. Kalnes, R.B. James, Env. Prog. 7 (1988) 185.
[18] R.G. Jones, Surf. Sci. 88 (1979) 367.
[19] J.C. Cook, E.M. McCash, Surf. Sci. 365 (1996) 573.
[20] N.J. Sack, L. Nair, T.E. Madey, Surf. Sci. 310 (1994) 63.
[21] M.A. Chesters, D. Lennon, Surf. Sci. 426 (1999) 92.
[22] R.J. Meyer, D.J. Safarik, C.T. Reeves, D.T. Allen, C.B. Mullins, J. Mol. Catal. A 167 (2001) 59.
[23] R.J. Meyer, C.T. Reeves, D.J. Safarik, D.T. Allen, C.B. Mullins, J. Vac. Sci. Technol. A, accepted for publication.
[24] M.C. Wheeler, D.C. Seets, C.B. Mullins, J. Chem. Phys. 105 (1996) 1572.
[25] B.A. Ferguson, C.T. Reeves, C.B. Mullins, J. Chem. Phys. 110 (1999) 11574.
[26] R. Koch, M. Borbonus, O. Haase, K.H. Rieder, Appl. Phys. A 55 (1992) 417.
[27] R. Koch, M. Borbonus, O. Haase, K.H. Rieder, Phys. Rev. Lett. 67 (1991) 3416.
[28] J. Kuntze, S. Speller, W. Heiland, Surf. Sci. 402 (1998) 764.
[29] C.M. Chan, M.A. Van Hove, W.H. Weinberg, E.D. Williams, Surf. Sci. 91 (1980) 440.
[30] C.M. Chan, M.A. Van Hove, Surf. Sci. 171 (1986) 226.
[31] W. Hetterich, W. Heiland, Surf. Sci. 210 (1989) 129.

[32] H. Bu, M. Shi, F. Masson, J.W. Rabalais, Surf. Sci. 230 (1990) L140.
[33] D.J. Auerbach, in: G. Scoles (Ed.), Atomic and Molecular Beam Methods, vol. 1, Oxford University Press, New York, 1988.
[34] P.A. Redhead, Vacuum 12 (1962) 203.
[35] R.J. Meyer, C.T. Reeves, D.J. Safarik, C.B. Mullins, unpublished results.
[36] R. Schennach, E. Bechtold, Surf. Sci. 380 (1997) 9.
[37] D.A. King, M.G. Wells, Surf. Sci. 29 (1972) 454.
[38] C.T. Rettner, L.A. DeLouise, D.J. Auerbach, J. Chem. Phys. 85 (1986) 1131.
[39] J.E. Davis, S.G. Karseboom, P.D. Nolan, C.B. Mullins, J. Chem. Phys. 105 (1996) 8362.
[40] C.B. Mullins, W.H. Weinberg, in: R.J. Madix (Ed.), Surface Reactions, Springer Series in Surface Sciences, vol. 43, Springer, Berlin, 1994.
[41] C.R. Arumainayagam, R.J. Madix, Prog. Surf. Sci. 38 (1991) 1.
[42] M.N.R. Ashfold, C.T. Rettner (Eds.), Dynamics of Gas–Surface Interactions, Royal Society of Chemistry, London, 1991.
[43] D.R. Lide, Handbook of Chemistry and Physics, 81st ed., CRC Press, Boca Raton, 2000.
[44] V.I. Minkin, O.A. Osipov, Y.A. Zhdanov, Dipole Moments in Organic Chemistry, Plenum Press, New York, 1970.
[45] W. Erley, Surf. Sci. 114 (1982) 47.
[46] D.E. Ibbotson, T.S. Wittrig, W.H. Weinberg, J. Chem. Phys. 72 (1980) 4885.
[47] E. Kirsten, G. Parschau, W. Stocker, K.H. Rieder, Surf. Sci. 231 (1990) L183;
H.T. Lorensen, Adsorbate Induced Structures and Self-diffusion on Platinum Surfaces, Ph.D. Thesis, Department of Physics, Technical University of Denmark, December 1999.
[48] T.S. Wittrig, P.D. Szuromi, W.H. Weinberg, J. Chem. Phys. 76 (1982).